

Supplementary Information

Two-dimensional fully-conjugated polymeric photosensitizers for advanced photodynamic therapy

Zhonghua Xiang^{1,2,3} ‡, Lin Zh⁴ ‡, Lei Qi⁴, Lu Yan⁴, Yuhua Xue⁴, Dan, Wang^{1,2},
Jian-Feng Chen^{1*}, and Liming Dai^{2,3,4*}

¹ State Key Laboratory of Organic-Inorganic Composites, Beijing University of Chemical Technology, Beijing 100029, China.

² Energy Institute, BUCT-CWRU International Joint Laboratory, Beijing University of Chemical Technology, Beijing 100029, China.

³ Centre of Advanced Science and Engineering for Carbon (Case4Carbon), Department of Macromolecular Science and Engineering, Case Western Reserve University, 10900 Euclid Avenue, Cleveland, OH 44106 (USA).

⁴ Institute of Advanced Materials for Nano-Bio Applications, School of Ophthalmology & Optometry, Wenzhou Medical University, Wenzhou 325027, China

‡ These authors contributed equally to this work.

^{*} Correspondence and requests for materials should be addressed to: J.-F. C (chenjif@mail.buct.edu.cn) and D.L. (email: lxdl15@case.edu).

1. Materials Synthesis and Characterization

1.1 Materials All reagents were obtained from commercial sources (Alfa Aesar, Sigma Aldrich) and used without further purification unless otherwise stated. Bis(1,5-cyclooctadiene)nickel(0) ($[\text{Ni}(\text{cod})_2]$) was purchased from J&K. 5,10,15,20-tetrakis- (4'-bromo-biphenyl-4-yl)-porphyrine (TBBPP) was purchased from Asta Tech (Chengdu). 1,5-Cyclooctadiene (cod) was dried over CaH_2 prior to use.

1.2 Characterizations

X-ray diffraction (XRD) measurements were performed with D/MAX 2000 X-ray diffractometer with Cu $K\alpha$ line ($\lambda=1.54178 \text{ \AA}$) as the incident beam. **FT-IR spectroscopy** was performed on an AC-80MHZ (Bruker) instrument with the wavenumber range of $400\text{-}4000 \text{ cm}^{-1}$. **Scanning electron microscopic (SEM)** images were obtained on a TESCAN VEGA 3 SEM instrument. **Transmission electron microscopic (TEM)** images were obtained on a Carl Zeiss AG - LIBRa 200 FE instrument. **Atomic force microscopy (AFM)** images were performed on an Agilent 5500 atomic force microscope. **UV-UV/visible absorption** of dilute solutions (0.1 mg mL^{-1}) of TBBPP, COP-P and COP-P- SO_3H in water was measured on a V-670 spectrophotometer. 1% N, N'-dimethylformamide (DMF) was added into the solutions of TBBPP and COP-P due to poor hydrophilicity of the two samples. **X-Ray Photoelectron Spectrometer (XPS)** was carried out with a PHI Versaprobe 5000 Scanning XPS instrument. **Contact angles** were measured with a dataphysics contact angle instrument. Each angel was calculated from the mean of five independent

measurements.

2. Determination of the Energy Levels of HOMO and LUMO

The energy levels of HOMO and LUMO were determined from electrochemical CV measurements according to the previously reported method.^(S1, S2) Briefly, the electrochemical measurements were performed in 0.1 M tetrabutylammonium hexafluorophosphate ([Bu₄N]PF₆) acetonitrile solution under the protection of dry N₂, using Pt wire as counter electrode, Ag/AgCl electrode as reference electrode and a glassy carbon electrode coated with the samples as the working electrode, respectively. The electrochemical potential was calibrated against ferrocene/ferrocenium (Fc/Fc⁺). The energy levels of the highest occupied (HOMO) and lowest unoccupied molecular orbital (LUMO) were then calculated according to the following equations:

$$\text{HOMO} = -e (E_{ox} + 4.38) \quad (\text{eV})$$

$$\text{LUMO} = -e (E_{red} + 4.38) \quad (\text{eV})$$

where E_{ox} is the onset oxidation potential versus Ag/AgCl, and E_{red} is the onset reduction potential versus Ag/AgCl.

3. Photodynamic Therapy Investigation

3.1 Culture of MDA-MD-231 cells

MDA-MD-231 cells were cultured in minimum essential media (MEM, Invitrogen) containing 10% fetal bovine serum (FBS, Invitrogen), penicillin (100 U mL⁻¹) and streptomycin (100 U mL⁻¹, Invitrogen), at 37 °C in a humidified 5% CO₂-containing atmosphere.

3.2 *In vitro* phototoxicity assay on tumor cells

Cell Viability: MTT Cell Proliferation and Cytotoxicity Assay kit (MTT, Beyotime) was used to determine the cell viability. The MDA-MD-231 cells were seeded in 96-well plates at a density of 5,000 cells/well and incubated for 24 hs. For the first group, the cells were cultured in an incubator with various concentrations (50, 100, 150 and 200 $\mu\text{g mL}^{-1}$) of COP-P-SO₃H nanoparticles. Cells cultured in medium without COP-P-SO₃H nanoparticles were used as negative controls. For the cells to be irradiated, they were exposure to the light at 710 nm for 10 min after 4 h of incubation, than both of the irradiated and non-irradiated cells were continually cultured for another 24 hs. For the non-irradiated cells, the adhering cells were cultured in an incubator with 0 or 100 $\mu\text{g mL}^{-1}$ of COP-P-SO₃H nanoparticles. After 4 h of incubation, the cells were exposure to light at 710 nm for 0, 5, 10, 15 and 20 mins (0 min cells were used as negative controls). Then, all the cells were continually cultured for another 24 hs. Following the method of the MTT assay, the optical density (OD) of each well at 570 nm was recorded by a SpectraMax M5 (Molecular Devices). Cell viability was expressed as the following percentage: $(\text{OD}_{\text{test}} - \text{OD}_{\text{blank}}) / (\text{OD}_{\text{negative}} - \text{OD}_{\text{blank}})$. OD_{blank} was the OD value of culture medium without cells.

Six parallel tests were conducted for each sample. All data were presented as the means and standard deviations (means \pm SD). The significance (p value) was calculated using unpaired, two-tailed Student's t-tests with unequal variance. The

symbol “*” denotes statistical significance (* \leq 0.05, ** \leq 0.01, *** \leq 0.001) compared with the negative control, and $p < 0.05$ was considered significant.

3.3 ROS generation assay for PDT systems

For the ROS assay-DCFH-DA, MDA-MB-231 cells were seeded at density 150×10^3 per mL in black 96 well plates with/without exposure to the light (5-20 minutes), or with/without dosage of COP-P-SO₃H particles (50-200 $\mu\text{g mL}^{-1}$) for 2 hours. Replace with 200 μL of 100 μM DCFH-DA (Sigma) (in culture medium) to each of the wells and incubated at 37 °C and 5 % CO₂ culture conditions for 30 minutes. After the aspiration of the DCFH-DA, 200 μL of medium was added to each of the wells and the intensity of the ROS probe was measured immediately as background, as well as incubator for 24 hours on a spectrophotometer (Molecular Devices, SpectraMax M2, SoftMax Pro 4.8, USA) with excitation at 485 nm, absorbance at 538 nm and peak at 530 nm, according to the manufacturer's procedure. The data are represented as the average of six \pm the standard deviation.

3.4 Singlet oxygen quantum yield

The comparison of the ability to generate singlet oxygen between COP-P-SO₃H and clinic material protoporphyrin IX (PPIX) was made by its quantum yield, which was measured according to the previously reported method with slight modification. (S3, S4) 1,3-diphenylisobenzofuran (DPBF) was employed as singlet oxygen indicator. The singlet oxygen quantum yield ϕ_{Δ} is given by:

$$\phi_{\Delta(\text{sample})} = \phi_{\Delta(\text{reference})} (S_{\text{sample}} / S_{\text{reference}}) (F_{\text{sample}} / F_{\text{reference}})$$

where subscripts sample and reference designate the COP-P-SO₃H complex and

PPIX, respectively, S stands for the slope of plot of the absorbance of DPBF (at 418 nm) vs. irradiation time. F stands for the absorption correction factor, which is given according to the following formula:

$$F = 1 - 10^{-OD}$$

where OD represents the optical density of COP-P-SO₃H sample at 710 nm and PPIX at 532 nm.

3.5 Use flow cytometry for analyses of DNA damage

Seeded MDA-MD-231 cells with 150 µg ml⁻¹ concentration of COP-P-SO₃H nanoparticles in eppendorf tubes and exposure to light at wavelength of 710 nm for 10 mins, then transferred cells to a 6-well plate at density of 1×10⁶ cells per well. For comparison, same amounts of cells were seeded to a 24-well plate dosage cell only with 150 µg ml⁻¹ concentration of COP-P-SO₃H nanoparticles without exposure to the light. After incubation for 2 hours, cells were harvested and immunofluorescence staining specific antibody, then following the manufactures protocol preparing for flow cytometry. Briefly, cells were fixing with 2% paraformaldehyde (USB corporation) for 10 minus. After washing by 1x PBS (Invitrogen) twice, cells were incubated with permeabilization buffer (R&D systems) 500 µL for 15 minutes. After washing, cells were stained with p-53-FITC (abcom), Rad 51 (abcom), XRCC4 and OGG1 in staining buffer (R&D system) 4 °C overnight. 2nd antibody (Alexa Fluor® 488 Goat Anti-Rabbit IgG or Alexa Fluor® 555 Goat Anti-Mouse IgG, Invitrogen) was then added for 45 minutes at room temperature and analyzed by flow cytometry (BD II LSR).

3.6 Statistical Evaluation

The data were analyzed by GraphPad Prism 5 software one-way analysis of variance (ANOVA), which were expressed as mean \pm standard deviation (SD) of two, three or six independent experiments. A p value < 0.05 was considered significant.

4. First-Principles Calculations

The screening the active sites for sulfonation were performed using the Vienna Atomic Simulation Package (VASP)(S5, S6) from Beijing University of Chemical Technology in China. Core electrons were replaced by the projector augmented wave (PAW) pseudo-potentials(S7) and the generalized gradient approximation of the Perdew, Burke, and Ernzerhof (PBE) functional (S8) was used for exchange and correlation. The cutoff energy for the plane-wave basis set was set to 500 eV in all calculations. The Gamma-point was used for the calculations. The convergence criteria for the electronic self-consistent iteration and the ionic relaxation loop were set to 10^{-4} eV and 0.2 eV/Å, respectively. A supercell of size $27.8 \times 27.8 \times 10 \text{ Å}^3$ was employed in the calculations. The adsorption energy E_{abs} was defined as the energy difference between the total energy of the -SO₃H group adsorbed on the COP system and the relaxed COP plus -SO₃H group.

The O₂ adsorption in COP-P-SO₃H was studied using a cluster approach by the Gaussian 03 program.(S9) The cluster used in this work is shown in the Supplementary Figure 14 and the dangling bonds were terminated by H atoms. The geometry optimization and the binding energies (B.E.'s) between O₂ and the studied cluster models were performed at the theoretical level of B3LYP/ 6-311g (2d, 2p). To

save calculating time, all the binding energies were obtained without performing basis set superposition error (BSSE) calculations, but it is valid to investigate the adsorption site at the same theory level, aiming at selecting the favorite adsorption site. The B.E. of the molecular complexes was computed by the following equation:(S10-13)

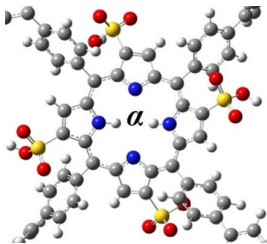
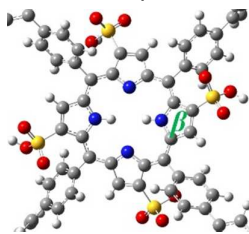
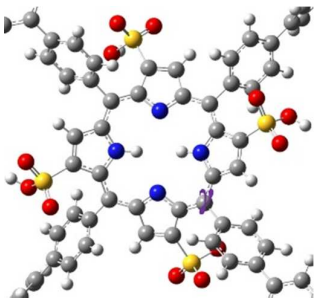
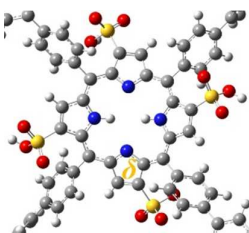
$$\text{B.E.} = E(\text{O}_2/\text{cluster}) - E(\text{cluster}) - E(\text{O}_2)$$


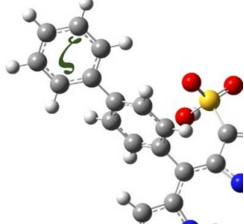
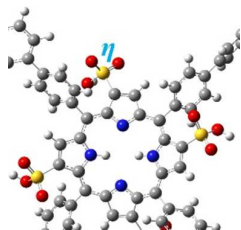
After screening the adsorption sites for O₂ in COP-P-SO₃H, we subsequently performed the molecular orbital calculations using the optimized adsorption site model at the theoretical level of B3LYP/ 6-311g (2d, 2p).

Table S1. Energy potentials and band gap derived from CVs for the monomer TBBPP, COP-P and COP-P-SO₃H.

	E_{ox}	E_{red}	HOMO (eV)	LUMO (eV)	Band gap (eV)
TBBPP	0.90	-0.64	-5.28	-3.74	1.54
COP-P	0.83	-0.64	-5.21	-3.74	1.47
COP-P-SO₃H	0.61	-0.46	-4.99	-3.92	1.07

Table S2. Summary of binding energies for the possible adsorption sites.

Adsorption sites	Description/ [Position before optimization] Position after optimization	Binding energy/ kcal mol ⁻¹
<p>Site α</p> 	<p>[On the top of porphyrine] The oxygen molecule moves close to top of pyrrolic N without H</p>	-4.67
<p>Site β</p> 	<p>[Site β-I; On the top of pyrrolic ring via parallel model] The oxygen molecule moves to the top of between two pyrrolic N atoms in porphyrine</p>	-8.11
	<p>[Site β-II; On the top of pyrrolic ring via vertical model] The oxygen molecule moves close to sulfonic acid group</p>	-5.10
<p>Site γ</p> 	<p>[On the top of methine bridges (=CH-)] The oxygen molecule moves to the top of between two pyrrolic N atoms in porphyrine</p>	-4.97
<p>Site δ</p> 	<p>[Site δ-I; On the top of pyrrolic ring via parallel model] The oxygen molecule moves to the top of pyrrolic N without H in porphyrin</p>	-8.60
	<p>[Site δ-II; On the top of pyrrolic ring via vertical model] The oxygen molecule moves to the</p>	-6.50

	top of pyrrolic N without H in porphyrin via parallel model	
Site ε 	[On the top of phenyl]	-5.31
Site ζ 	[On the top of phenyl]	-4.15
Site η 	[Around sulfonic acid group]	-5.12

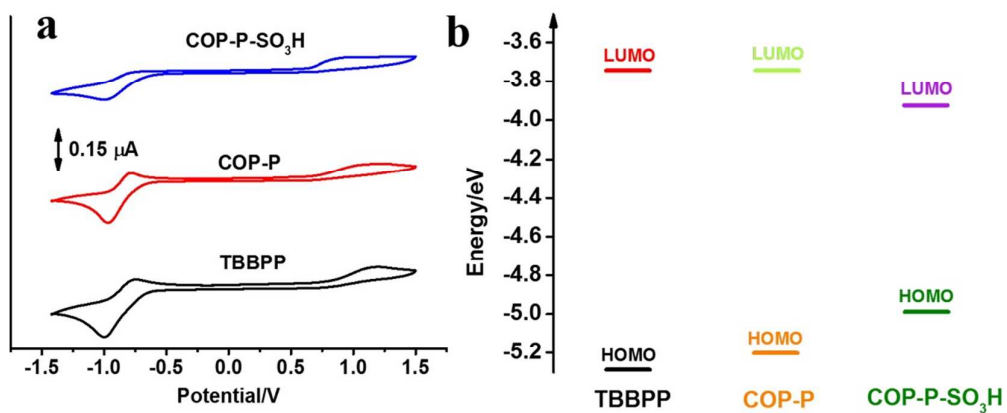


Figure S1. **a**, CV curves of TBBPP, COP-P and COP-P-SO₃H on glassy carbon electrode at a potential sweep rate of 0.05 V s⁻¹ in an acetonitrile solution of 0.1 M [Bu₄N]PF₆ at room temperature under the protection of dry N₂. **b**, Energy levels for TBBPP, COP-P and COP-P-SO₃H.

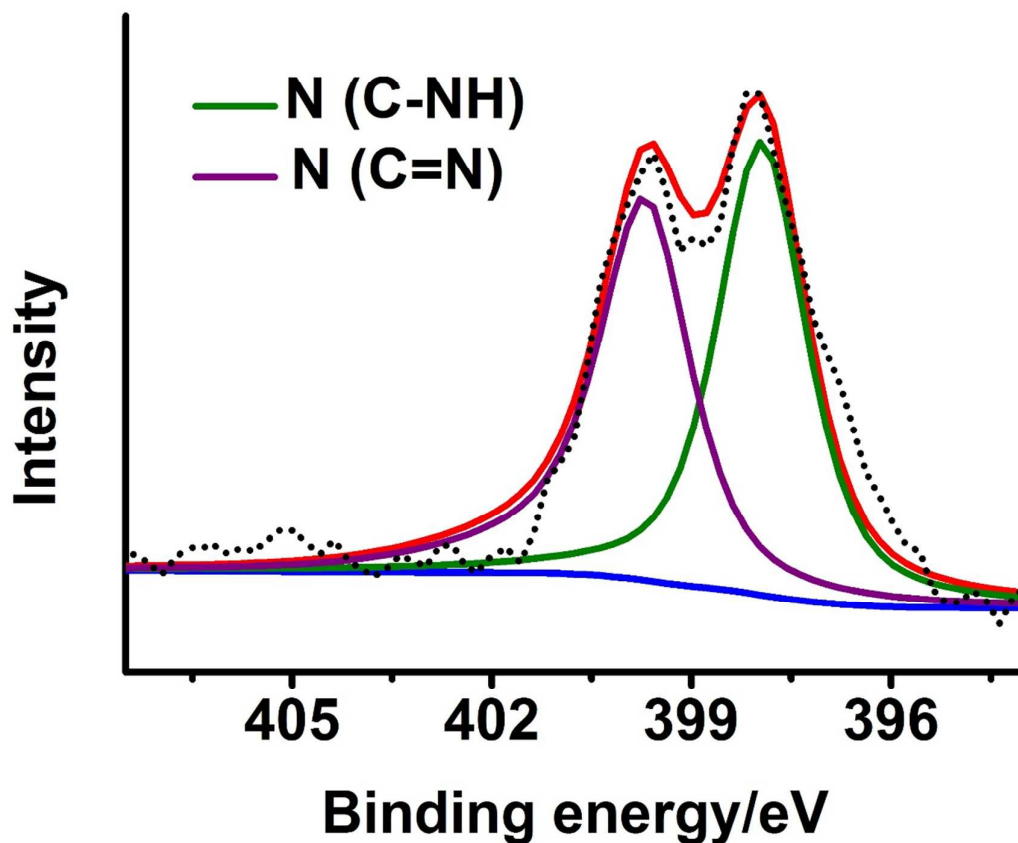


Figure S2. High-resolution XPS N1S spectrum of the COP-P-SO₃H. The N 1s peak can be deconvoluted into two Lorentzian peaks, which can be fitted into two different components corresponding to the pyrrolic N without H (397.7 eV, purple line) and pyrrolic N with H atoms (399.8 eV, olive line),(S14) respectively. The ratio of two peak areas is close to 1:1, suggesting the porphyrin ring skeletons were reserved after sulfonation with chlorosulfonic acid and the sulfonic acid groups do not connect with the pyrrolic N.

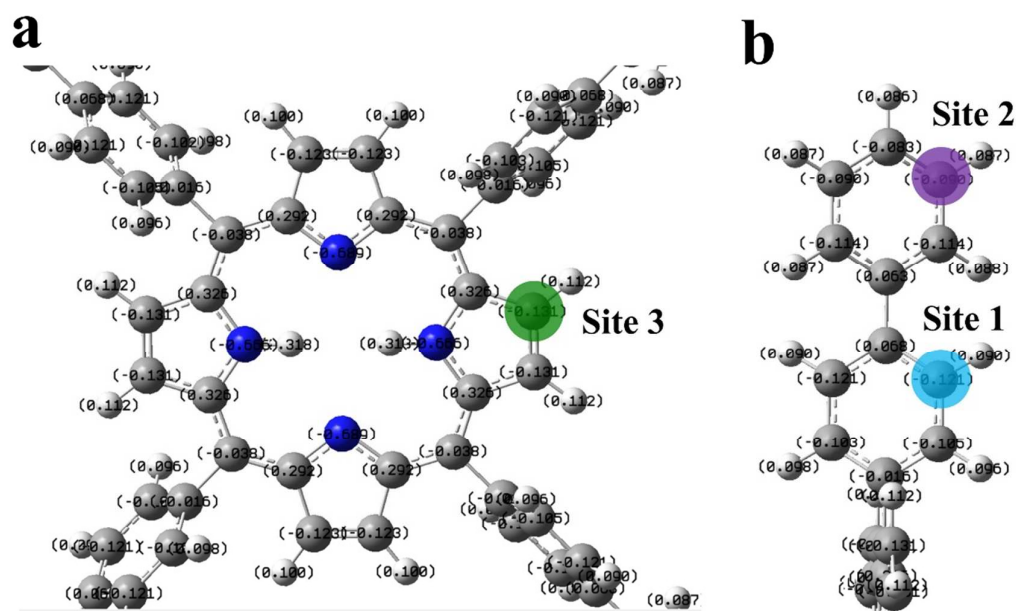


Figure S3. The charge distribution for COP-P cluster: **a**, for porphyrine and **b**, for two phenyl groups connected with porphyrine at the theoretical level of B3LYP/ 6-311g (2d, 2p). The calculations suggest there are mainly three kinds of active sites for sulfonation, localizing around the pyrrolic C and phenyl C (shown in green, cyan and purple shadow). Since the cluster for COP-P possesses centrosymmetric structure, here we just show the active sites in one direction and the active sites in symmetry positions are equal during sulfonation process.

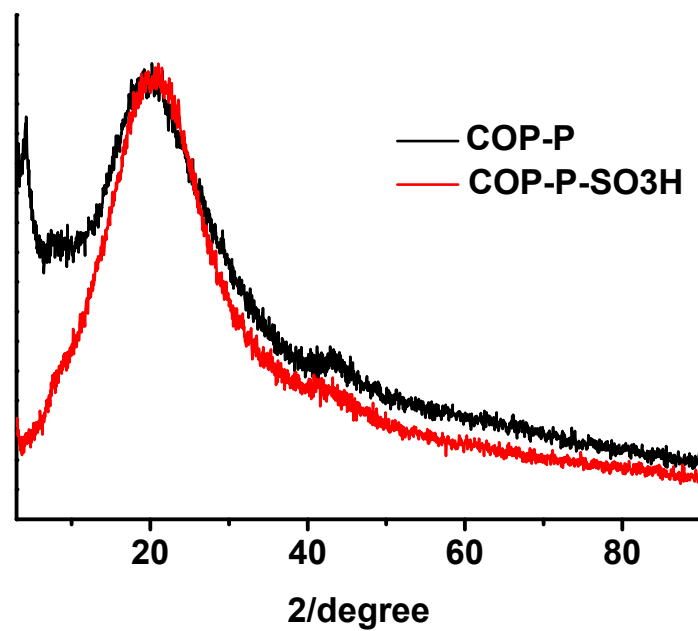


Figure S4. The XRD spectra of COP-P and COP-P-SO₃H.

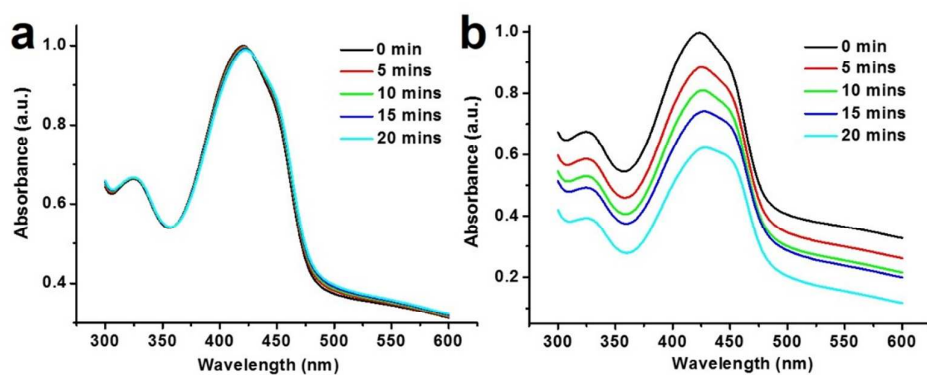


Figure S5. Optical absorption spectra at different photoexcited times measured for DPBF under irradiation with a 710-nm laser beam: **a**, without and **b**, with COP-P-SO₃H.

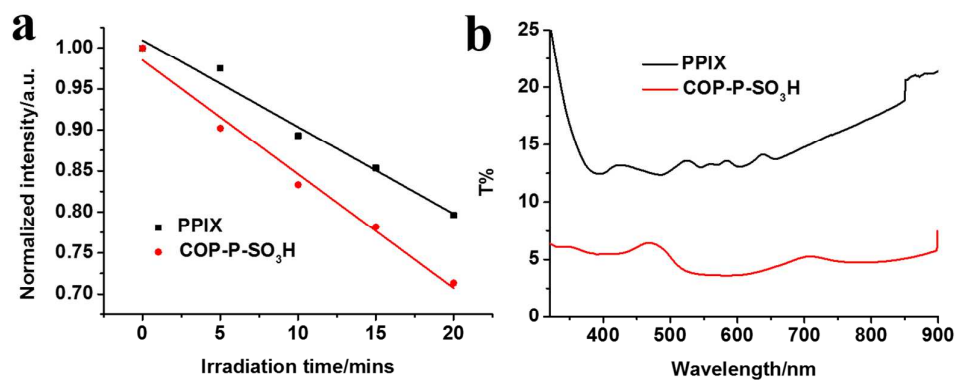


Figure S6. a, The plots for the absorbance of PPIX-mediated DPBF (at 418 nm) and COP-P-SO₃H mediated DPBF (at 418 nm) vs. irradiation time. **b**, The transmittance spectra for PPIX and COP-P-SO₃H.

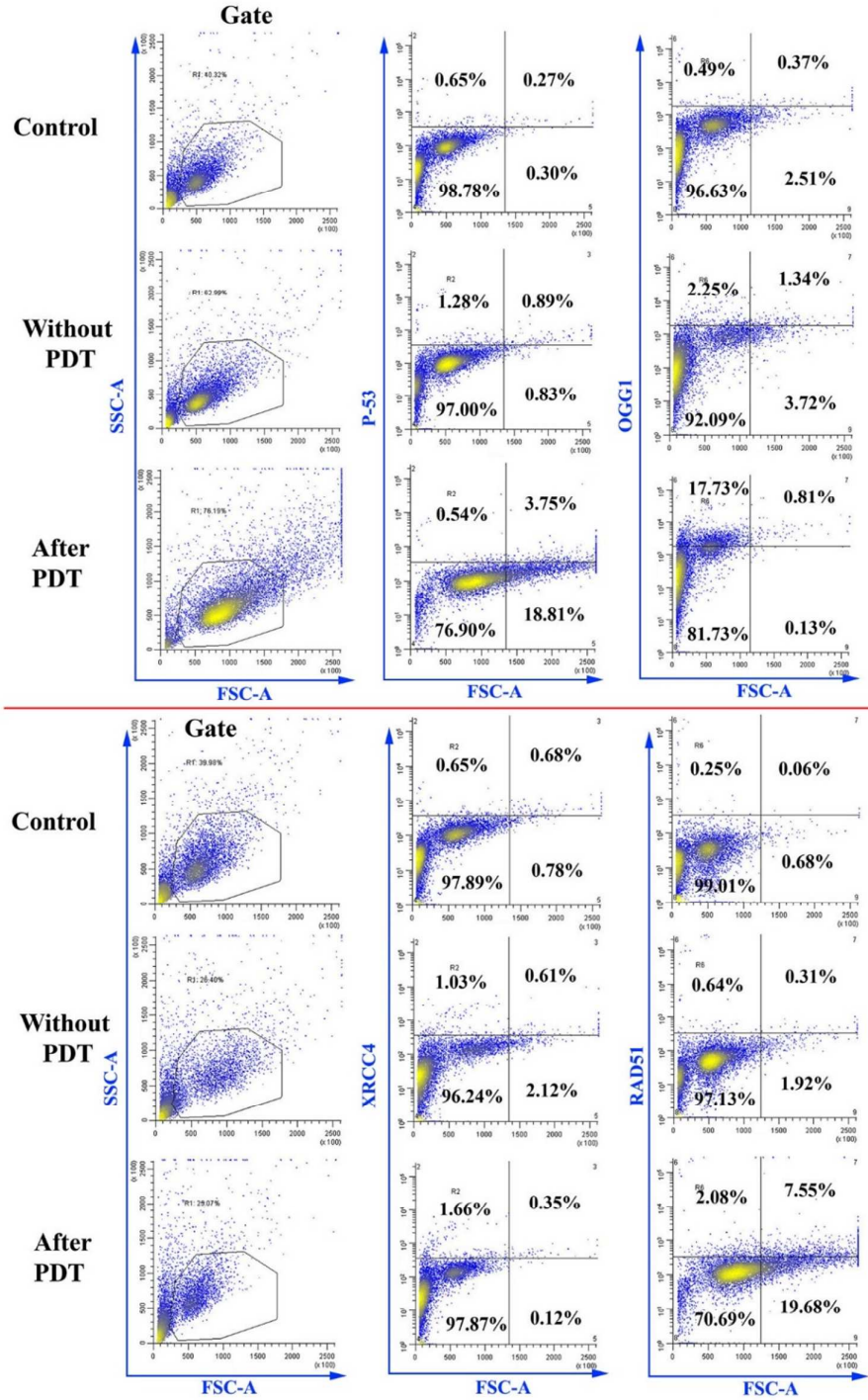


Figure S7. Flow cytometric analysis for COP-P-SO₃H-mediated PDT. Cells were stained with p-53-FITC, Rad 51, XRCC4 and OGG1 antibodies in staining buffer at 4⁰C overnight. Add 2nd antibody (Alexa Fluor® 488 Goat Anti-Rabbit IgG or Alexa Fluor® 555 Goat Anti-Mouse IgG), incubated at room temperature for about 45 minutes, then analyze by flow cytometry.

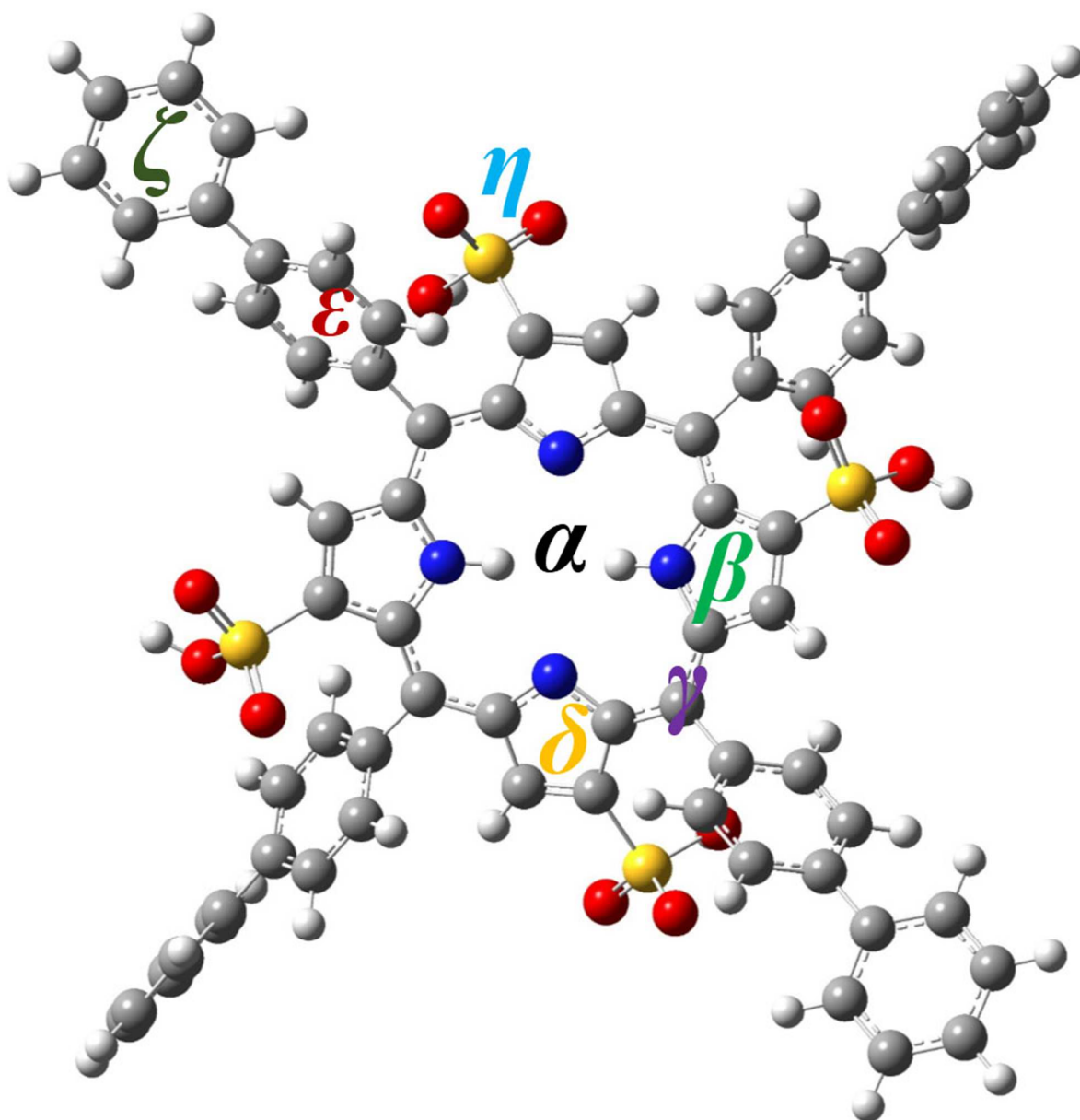


Figure S8. The adsorption sites for O₂ in the COP-P-SO₃H cluster. Site α , β , γ , δ and ϵ refer to the position around four N atoms in the porphyrin ring. C gray, H white, N blue, S yellow and O red.

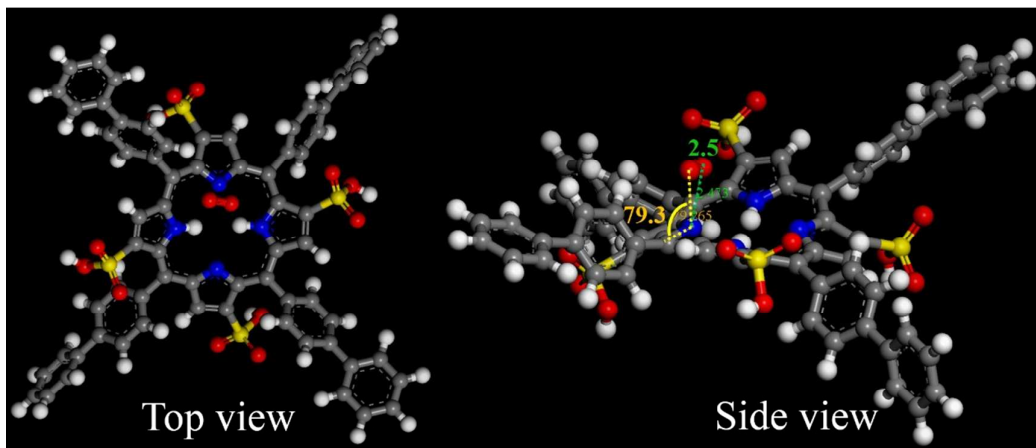


Figure S9. Optimized adsorption site α with B.E. = -4.67 kcal mol⁻¹ of O₂ molecule on the COP-P-SO₃H cluster. C, O, N, H and S atoms are shown as gray, red, blue, white and yellow balls. The measured distance is presented in angstrom, and the measured angle is presented in degree.

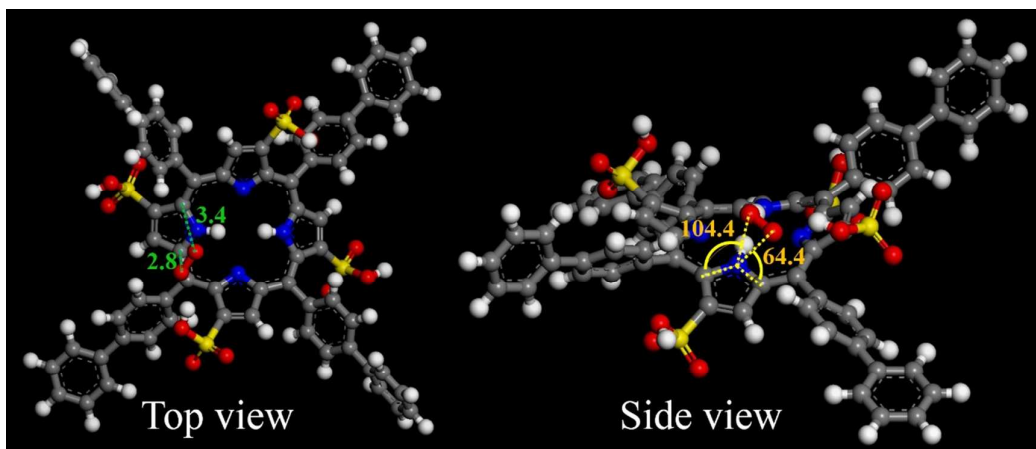


Figure S10. Optimized adsorption site β -I with B.E. = -8.11 kcal mol⁻¹ of O₂ molecule on the COP-P-SO₃H cluster. C, O, N, H and S atoms are shown as gray, red, blue, white and yellow balls. The measured distance is presented in angstrom, and the measured angle is presented in degree.

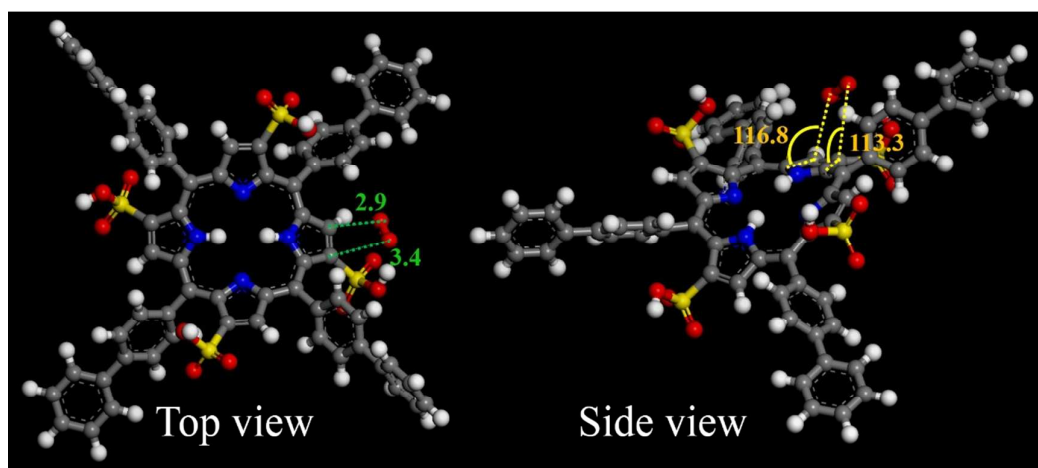


Figure S11. Optimized adsorption site β -II with B.E. = $-5.10 \text{ kcal mol}^{-1}$ of O_2 molecule on the COP-P- SO_3H cluster. C, O, N, H and S atoms are shown as gray, red, blue, white and yellow balls. The measured distance is presented in angstrom, and the measured angle is presented in degree.

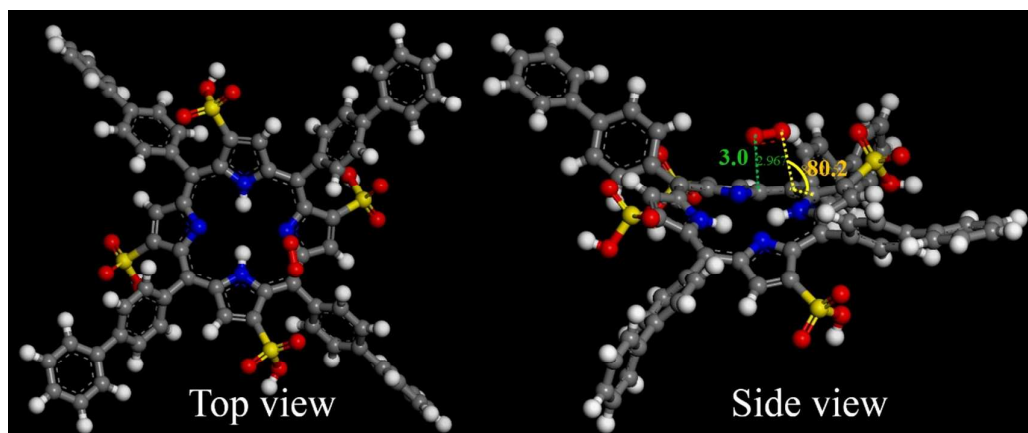


Figure S12. Optimized adsorption site γ with B.E. = $-4.97 \text{ kcal mol}^{-1}$ of O_2 molecule on the COP-P- SO_3H cluster. C, O, N, H and S atoms are shown as gray, red, blue, white and yellow balls. The measured angle is presented in degree.

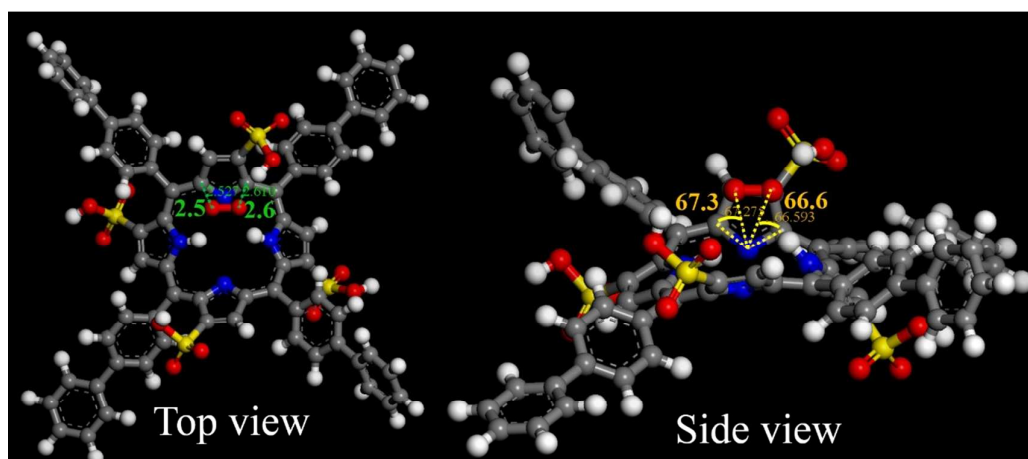


Figure S13. Optimized adsorption site δ -I with B.E. = $-8.60 \text{ kcal mol}^{-1}$ of O_2 molecule on the COP-P-SO₃H cluster. C, O, N, H and S atoms are shown as gray, red, blue, white and yellow balls. The measured angle is presented in degree.

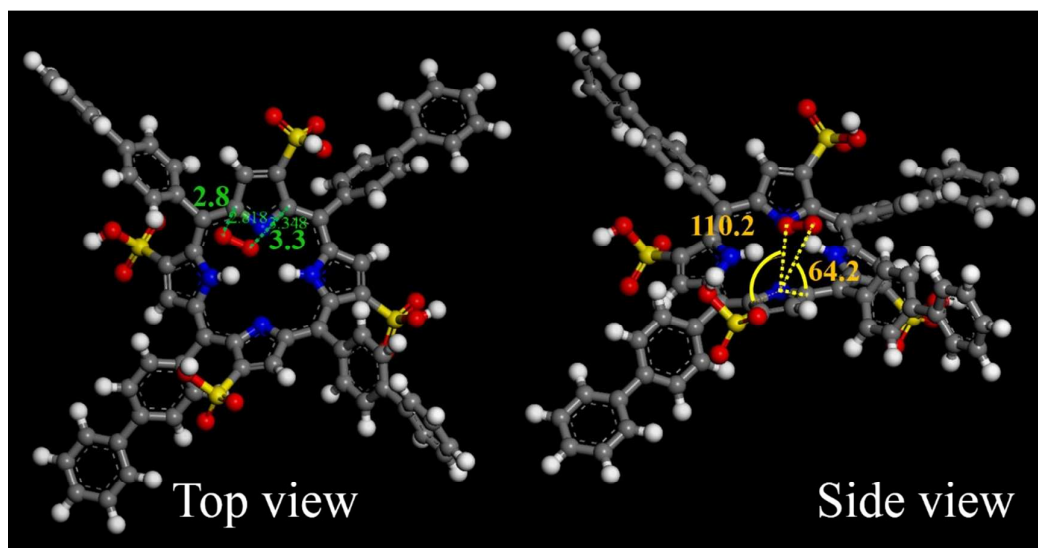


Figure S14. Optimized adsorption site δ -II with B.E. = $-6.50 \text{ kcal mol}^{-1}$ of O_2 molecule on the COP-P-SO₃H cluster. C, O, N, H and S atoms are shown as gray, red, blue, white and yellow balls. The measured angle is presented in degree.

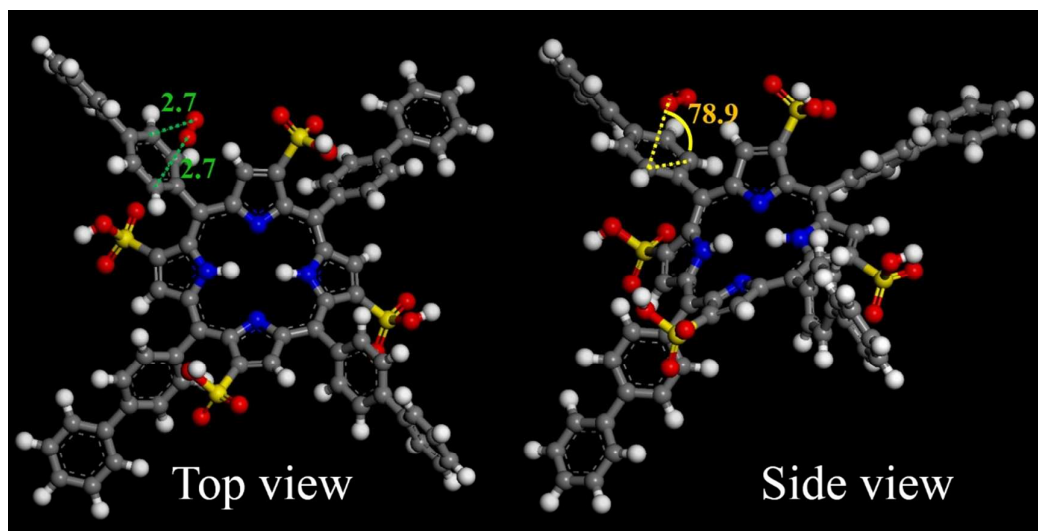


Figure S15. Optimized adsorption site ε with B.E. = -5.31 kcal mol⁻¹ of O_2 molecule on the COP-P-SO₃H cluster. C, O, N, H and S atoms are shown as gray, red, blue, white and yellow balls. The measured distance is presented in angstrom, and the measured angle is presented in degree.

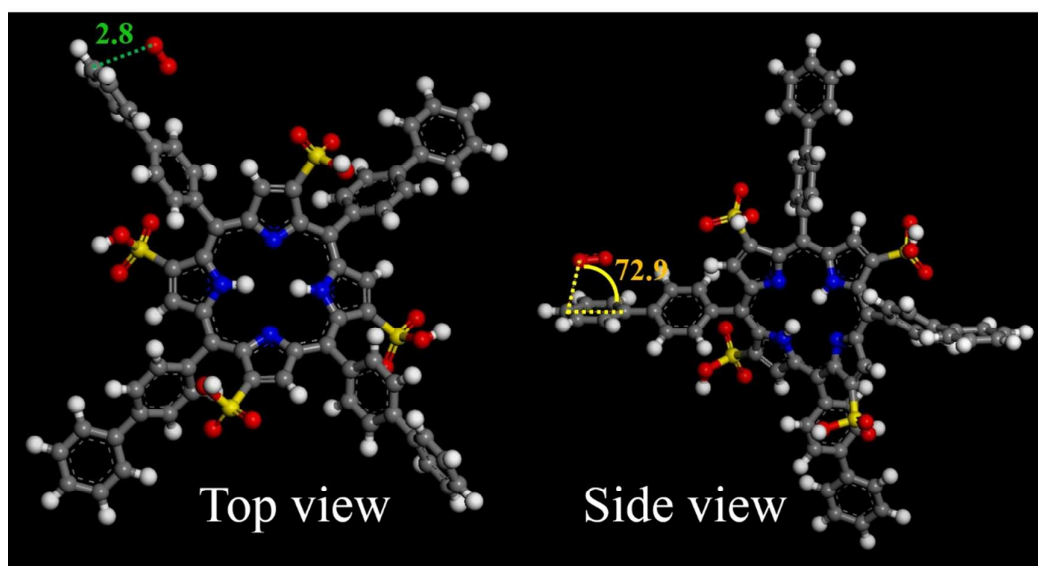


Figure S16. Optimized adsorption site ζ with B.E. = -4.15 kcal mol⁻¹ of O_2 molecule on the COP-P-SO₃H cluster. C, O, N, H and S atoms are shown as gray, red, blue, white and yellow balls. The measured distance is presented in angstrom, and the measured angle is presented in degree.

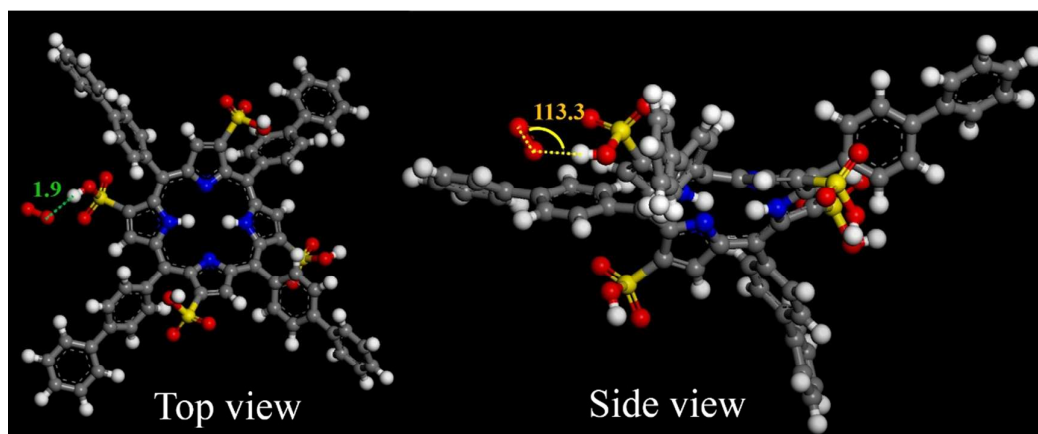


Figure S17. Optimized adsorption site η with B.E. = $-5.12 \text{ kcal mol}^{-1}$ of O_2 molecule on the COP-P-SO₃H cluster. C, O, N, H and S atoms are shown as gray, red, blue, white and yellow balls. The measured distance is presented in angstrom, and the measured angle is presented in degree.

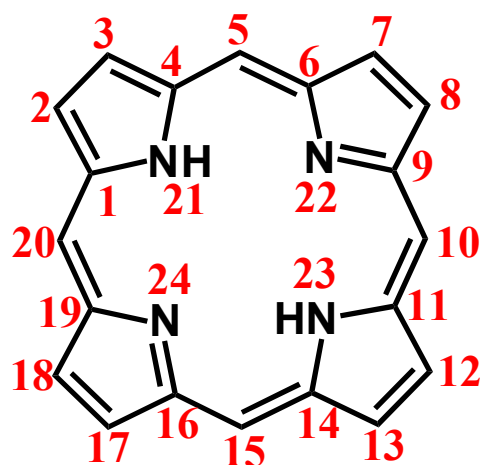


Figure S18. The atom numbers for porphyrine ring in this study.

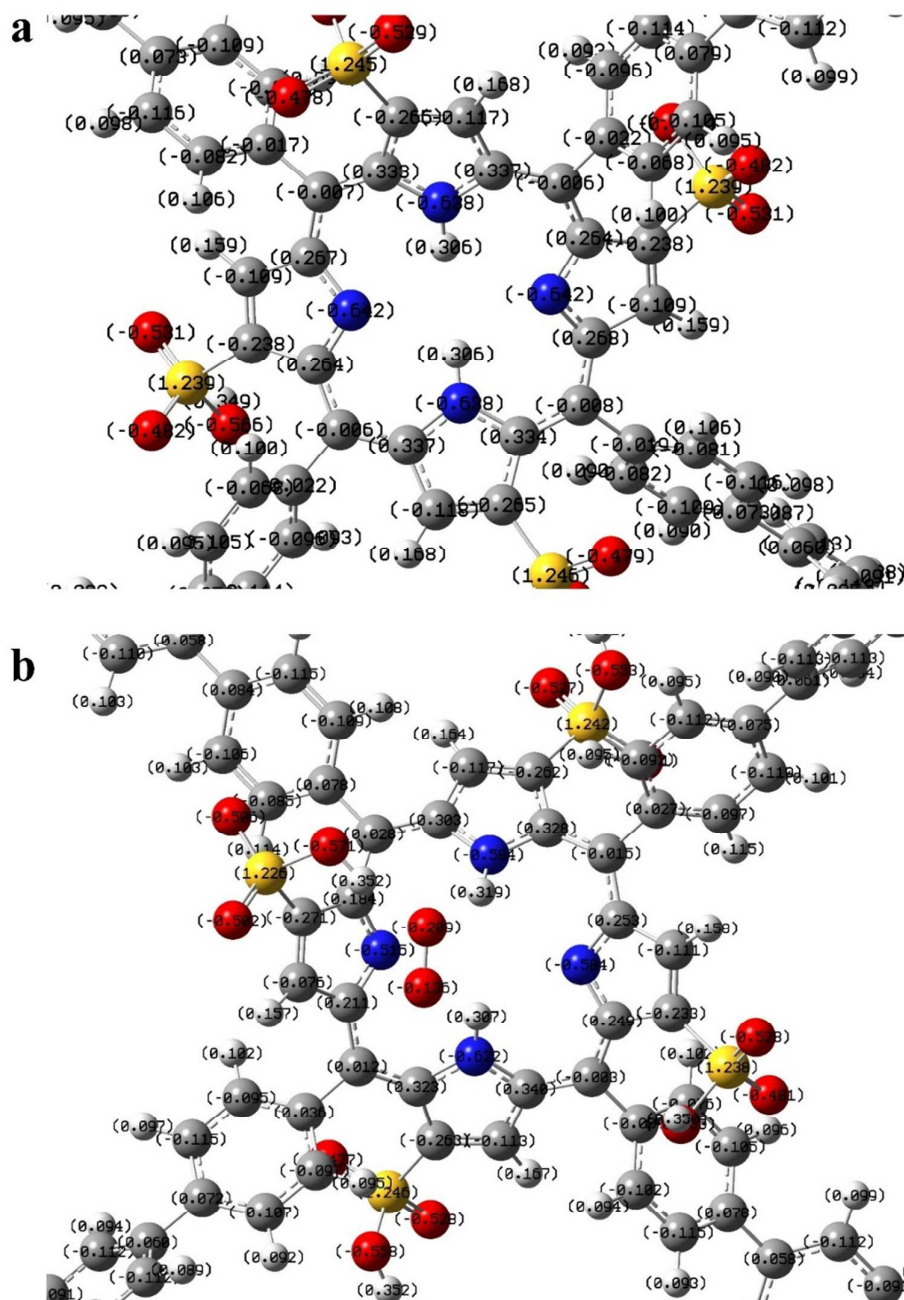


Figure S19. **a**, The calculated charge density distribution for the instinct COP-P cluster. **b**, The calculated charge density distribution for the COP-P-SO₃H after adsorbing O₂. As clearly shown, the porphyrine in COP-P-SO₃H plays a key role in the charge transfer after adsorbing oxygen molecule.

References

- S1. J. B. You, L. T. Dou, K. Yoshimura, T. Kato, K. Ohya, T. Moriarty, K. Emery, C. C. Chen, J. Gao, G. Li, Y. Yang, A Polymer Tandem Solar Cell With 10.6% Power Conversion Efficiency. *Nat. Commun.* **4**, 1446 (2013).
- S2. Q. J. Sun, K. Park, L. M. Dai, Liquid Crystalline Polymers for Efficient Bilayer-Bulk-Heterojunction Solar Cells. *J. Phys. Chem. C* **113**, 7892-7897 (2009).
- S3. J. Tian, L. Ding, H.-J. Xu, Z. Shen, H. Ju, L. Jia, L. Bao, J.-S. Yu, Cell-Specific And Ph-Activatable Rubyrin-Loaded Nanoparticles for Highly Selective Near-Infrared Photodynamic Therapy Against Cancer. *J. Am. Chem. Soc.* **135**, 18850-18858 (2013).
- S4. N. Adarsh, R. R. Avirah, D. Ramaiah, Tuning Photosensitized Singlet Oxygen Generation Efficiency of Novel Aza-BODIPY Dyes. *Org. Lett.* **12**, 5720-5723 (2010).
- S5. G. Kresse, J. Furthmüller, Efficient iterative schemes for ab initio total-energy calculations using a plane-wave basis set. *Phys. Rev. B* **54**, 11169 (1996).
- S6. G. Kresse, J. Furthmüller, Efficiency of ab-initio total energy calculations for metals and semiconductors using a plane-wave basis set. *Comp. Mater. Sci.* **6**, 15-50 (1996).
- S7. P. E. Blöchl, Projector augmented-wave method. *Phys. Rev. B* **50**, 17953 (1994).
- S8. J. P. Perdew, K. Burke, M. Ernzerhof, Generalized gradient approximation made simple. *Phys. Rev. Lett.* **77**, 3865 (1996).
- S9. M. J. Frisch, G. W. Trucks, H. B. Schlegel, G. E. Scuseria, M. A. Robb, J. R. Cheeseman, J. A. Montgomery, Jr., T. Vreven, K. N. Kudin, J. C. Burant, *Gaussian 03*, Revision C.02, Gaussian, Inc., Wallingford CT (2004).
- S10. Z. H. Xiang, D. P. Cao, J. H. Lan, W. C. Wang, D. P. Broom, Multiscale Simulation And Modelling of Adsorptive Processes for Energy Gas Storage And Carbon Dioxide Capture in Porous Coordination Frameworks. *Energy Environ. Sci.* **3**, 1469-1487 (2010).
- S11. Z. H. Xiang, S. H. Leng, D. P. Cao, Functional Group Modification of Metal-Organic Frameworks For CO₂ Capture. *J. Phys. Chem. C* **116**, 10573-10579 (2012).
- S12. Z. H. Xiang, J. H. Lan, D. P. Cao, X. H. Shao, W. C. Wang, D. P. Broom, Hydrogen Storage in Mesoporous Coordination Frameworks: Experiment And Molecular Simulation. *J. Phys. Chem. C* **113**, 15106-15109 (2009).
- S13. Z. H. Xiang, D. P. Cao, L. Huang, J. L. Shui, M. Wang, L. M. Dai, Nitrogen-Doped Holey Graphitic Carbon from 2D Covalent Organic Polymers for Oxygen Reduction. *Adv. Mater.* **26**, 3315-3320 (2014).
- S14. A. Ghosh, J. Fitzgerald, P. G. Gassman, J. Almlof, Electronic Distinction Between Porphyrins And Tetraazaporphyrins. Insights from X-Ray Photoelectron Spectra of Free Base Porphyrin, Porphyrazine, And Phthalocyanine Ligands. *Inorg. Chem.* **33**, 6057-6060 (1994).